J. Phys. B: At. Mol. Phys. **18** (1985) 1409-1418. Printed in Great Britain

Absolute electron impact emission cross section of the He^+ $2^2P \rightarrow 1^2S$ line at 304 Å produced by simultaneous ionisation–excitation

J L Forand, K Becker and J W McConkey†

Department of Physics, University of Windsor, Windsor, Ontario, Canada N9B 3P4

Received 24 September 1984, in final form 20 November 1984

Abstract. A simple and straightforward approach to an absolute emission cross section measurement of the He^+ $2^2P \rightarrow 1^2S$ line at 304 Å following the simultaneous ionisation-excitation of He by electron impact is presented. The undispersed He and He^+ impact radiation in the extreme ultraviolet (XUV) region ($\lambda \leqslant 600$ Å) is detected by a channel electron multiplier after passing through an XUV filter. A 304 Å emission cross section of $(6.2 \pm 1.7) \times 10^{-19}$ cm^2 at 200 eV impact energy is extracted utilising the known He cross sections, the measured He/He^+ ratio and the wavelength-dependent transmission of the XUV filter and quantum yield of the photon detector. In the regime of high impact energies the emission cross section is found to be inversely proportional to the incident electron energy as expected for the optically forbidden two-electron simultaneous ionisation-excitation process.

1. Introduction

The ionisation of atoms by electron impact has been studied extensively since the early days of electron collision physics. Most of this work has been focused on the single ionisation of an atom into the ground state of the resulting ion. In particular, the electron impact ionisation of helium has been thoroughly investigated, since its simple atomic structure makes it a preferred candidate for very stringent comparisons between experiment and theory. By comparison, the single-step ionisation-excitation of atoms by electron impact has not received nearly as much attention in the literature. Since two atomic electrons are involved simultaneously, cross sections for these processes are comparatively small, and the theoretical treatment is more complicated.

In the case of He, only a few transitions have been studied with the main emphasis on cross section and polarisation measurements of the He^+ $n = 4 \rightarrow n = 3$ manifold at 4686 Å (see figure 1). A summary of these results can be found in the review article by Heddle and Keesing (1968), and further discussion has been given very recently by Shemansky *et al* (1984). Information about the excitation of individual l states can only be obtained by utilising the different lifetimes of these states, since the He^+ energy levels are practically degenerate with respect to l for a given n. Sutton and Kay (1974) performed a time-resolved measurement of the $4l$-sublevel cross sections which disagreed with the theoretical predictions of Lee and Lin (1965). Reliable data on the prominent vacuum ultraviolet (VUV) lines of He^+ (1640, 1215 and 304 Å) are even

† NASA Senior Research Associate, Jet Propulsion Laboratory, Pasadena, during 1983-84.

0022-3700/85/071409+10$02.25

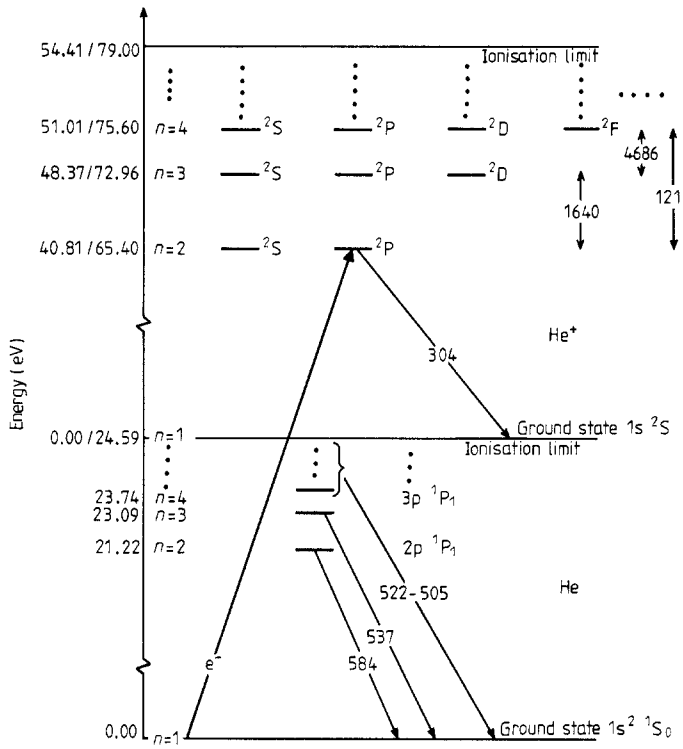

Figure 1. Partial energy level diagram of He and He^+. The two energy scales start from the ground state of He and He^+, respectively. The energy values have been taken from Stringanov and Sventitiskii (1968). The wavelengths of the most prominent emission lines are given in ångströms. Note that the He^+ energy levels are practically degenerate with respect to the orbital angular momentum quantum number l for a given principle quantum number n. The spin-orbit splitting of the He^+ states with $l \neq 0$ is very small (0.7 meV or less) and has been neglected.

more scarce. Moustafa Moussa and de Heer (1967) reported emission cross sections for these lines; however, the accuracy of their data at 1640 and 304 Å is questionable, since they estimated the quantum yield of their monochromator-detector system at those wavelengths by extrapolation over many hundreds of ångströms. When the same group remeasured the 304 Å cross section 14 years later using a photoionisation chamber as an absolute radiation detector, they found a value that was 50% higher (Bloemen *et al* 1981). Recently Shemansky *et al* (1984) have presented new data for the 1640 Å line.

The emission cross section of the He^+ 304 Å line produced in the simultaneous electron impact ionisation-excitation of He is of experimental and theoretical interest. It can be used, if accurately known, for convenient and easily reproducible calibration of optical instrumentation in the extreme ultraviolet, where calibration standards are scarce. (Of course, other problems inherent in absolute cross section measurements, such as target density determination, must still be carefully addressed.) Secondly, since the line is emitted in the only optically allowed decay route from $n = 2$ to $n = 1$, the transition is not affected by the (nearly) l degeneracy of the He^+ energy levels (see figure 1). Thus the 304 Å emission cross section provides a very direct comparison

between experiment and theory. Finally, the process should be accessible to *ab initio* calculations, since it represents the simplest case of simultaneous ionisation-excitation by electron impact.

In the present paper we report a different approach for determining an absolute emission cross section of the He^+ $2^2P \rightarrow 1^2S$ line at 304 Å produced by electron impact on He. A straightforward arrangement was employed, where the unresolved $He + He^+$ radiation produced by electrons incident on He is detected by a channel electron multiplier after passing through an extreme ultraviolet (XUV) filter. Cross sections for the He^+ emissions, in particular for the 304 Å line, are extracted from the total signal by utilising the well known emission cross sections for the He resonance lines ($n^1P_1 \rightarrow 1^1S_0$, 584-505 Å), (van Eck and de Jongh 1970, Donaldson *et al* 1972, Westerveld *et al* 1979), the transmission properties of the XUV filter at the various wavelengths and the (wavelength-dependent) response of the photon detector. The range of incident energies was extended to 1 keV in order to study the high-energy behaviour of the cross section and thus gain information about the nature of the excitation mechanism. In the high-energy regime, optically allowed excitation processes are characterised by a $\ln E/E$ dependence (Bethe 1930), whereas a collision-induced optically forbidden transition leads to a more rapid $1/E$ decline of the cross section.

2. Experimental

A schematic diagram of the apparatus is given in figure 2. The crossed electron-gas beam arrangement has been described in previous publications (Donaldson *et al* 1972, Becker and McConkey 1984). The undispersed radiation produced by the inelastic electron-helium collisions is detected by a Galileo Electro-Optics 4039C channeltron connected to a standard pulse counting system after passing through a Luxel TF 101 extreme ultraviolet filter (cf left-hand side of figure 2). The transmission properties of the filter, which consists of a 1500 Å Al:Si film with a 270 Å carbon overcoat, were measured at various wavelengths using a 0.5 m Seya-Namioka grating monochromator and were found to be in excellent agreement with the specifications given by the manufacturer. Alternatively, the monochromator (for details see Donaldson *et al* 1972, Becker *et al* 1983) could be employed to isolate the 304 Å radiation from adjacent He and He^+ emissions (cf right-hand side of figure 2). This set-up was used for relative excitation function measurements in the high-energy regime above 300 eV, where the

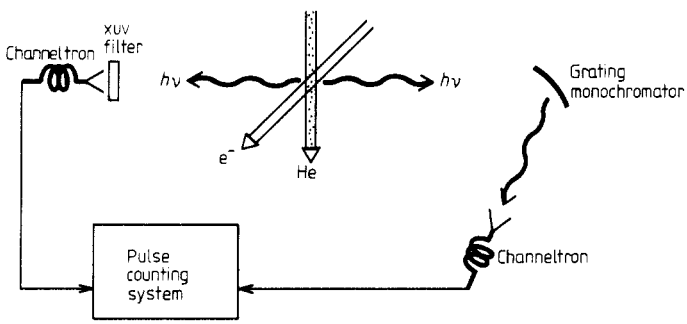

Figure 2. Schematic diagram of the two experimental arrangements. Details are given in the text.

direct detection of the undispersed impact radiation turned out to be difficult. The XUV filter, which was mounted a few mm in front of the entrance cone of the channeltron, could not be electrically biased and so the channeltron cone had to be kept at a negative bias voltage relative to the earthed interaction region to prevent the detection of stray electrons. When this bias voltage exceeded 300 V, field penetration effects into the interaction region began to affect the shape of the measured excitation function. We usually worked at a bias voltage of −250 V which in turn limited the incident electron energy with this arrangement to about 300 eV. Below 300 eV, excellent agreement was found between the excitation function measured for the spectrally isolated 304 Å line and that extracted from the measurement of the undispersed signal.

3. Results and discussion

3.1. The low-energy region (threshold to 300 eV)

The rapidly declining transmittance of the XUV filter above 600 Å restricts the detectable impact radiation to contributions from the He $n^1P_1 \rightarrow 1^1S_0$ resonance series and from the $He^+ n^2P \rightarrow 1^2S$ sequence. The measured excitation function for the combined He + He^+ emissions is shown in figure 3 (open circles) for impact energies up to 300 eV. Low background pressures below approximately 6×10^{-6} Torr in the collision chamber were used, since the He fraction of the signal is known to be seriously affected by radiation trapping (Heddle and Lucas 1963). Two measurements taken at background pressures of 2×10^{-6} and 5.5×10^{-6} Torr were combined for the curve displayed in figure 3, but only after the two measurements were found to be proportional over the

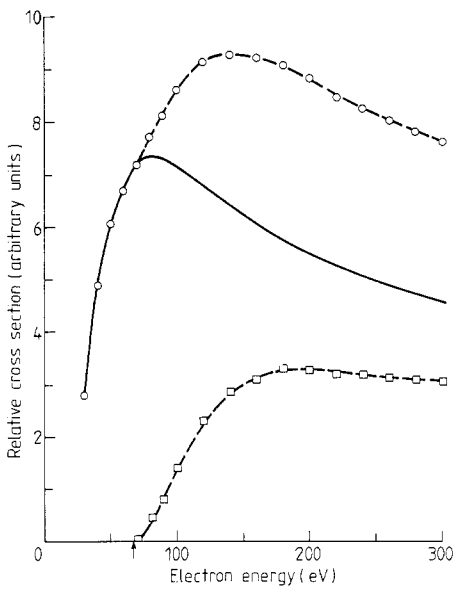

Figure 3. Relative excitation function of the combined He + He^+ extreme ultraviolet emissions ($\lambda \leq 600$ Å) as a function of electron impact energy (○). The full curve represents the constructed excitation function of the He contribution (details are given in the text). The difference between these two curves gives the relative excitation function of the He^+ $n^2P \rightarrow 1^2S$ emissions (□).

whole energy range with a proportionality factor very close to the pressure ratio. With typical electron beam currents between 25–30 μA and a data accumulation time of 20 s per energy point, counting statistics of 1% or better were achieved.

The full curve in figure 3 represents the excitation function of the He contribution in the total signal. Averaged data from the measurements by van Eck and de Jongh (1970), Donaldson *et al* (1972) and Westerveld *et al* (1979) were used. The strong polarisation of the He resonance radiation was taken into account on the basis of the polarisation data summarised in the work of Westerveld *et al* (1979). The He excitation function was normalised to our data at 50 eV. (The lowest threshold for He^+ emission is 65.4 eV, see figure 1.) Note the excellent agreement between the constructed He excitation function and the measured curve below 65 eV. By subtracting the He contribution from the measured excitation function, a curve representing the radiation arising from the $n^2P \rightarrow 1^2S$ transitions of He^+ is obtained (open squares). The He^+ cross section displays a broad maximum around 200 eV and falls off gradually towards higher impact energies. This shape is very similar to the one given in the work of Moustafa Moussa and de Heer (1967) for the 304 Å line and it also agrees well with a very recent measurement of the He^+ 1640 Å $n = 3 \rightarrow n = 2$ cross section (Shemansky *et al* 1984). Details of the near-threshold region are shown in figure 4. This curve was obtained by sweeping over the 50–100 eV energy range for several hours and subsequently subtracting the He contribution as described above. The onset of the 304 Å $2^2P \rightarrow 1^2S$ line at 65.4 eV was used to calibrate the energy scale. Note that there is only a slight indication of an upward trend around 75 eV which would correspond to the onset of emissions from higher n states. This confirms previous measurements and calculations (Moustafa Moussa and de Heer 1967, Shemansky *et al* 1984) which indicated that the cross section for exciting the higher ^2P states declines rapidly with increasing principle quantum number.

3.1.1. Normalisation procedure. The relative He^+ excitation function of figure 3 can be put on an absolute scale by utilising the known cross section for the He resonance

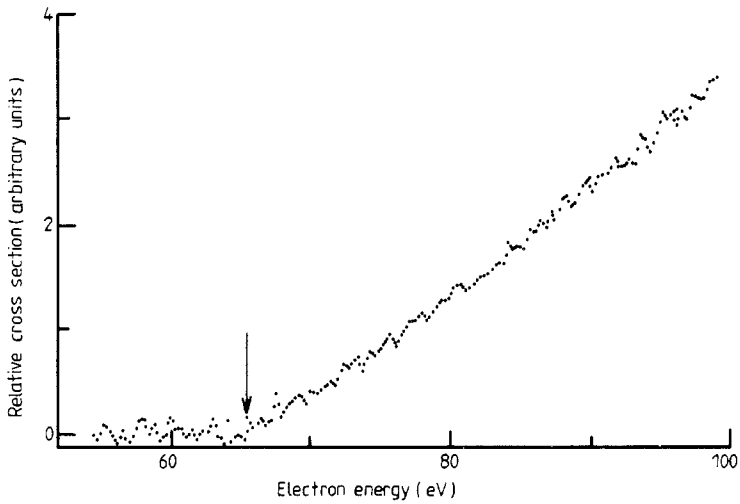

Figure 4. Near-threshold region of the He^+ $n^2P \rightarrow 1^2S$ excitation function. The arrow indicates the 65.4 eV threshold for emission of the $2^2P \rightarrow 1^2S$ line at 304 Å.

lines, the measured He/He^+ ratio and the wavelength-dependent transmission properties of the XUV filter and quantum yield of the photon detector. The various steps involved in the normalisation, which was made at an impact energy of 200 eV, are described in detail below.

The absolute He resonance line data have been taken as the average of the cross sections (cascade included, corrected for polarisation) given in the work of van Eck and de Jongh (1970), Donaldson *et al* (1972) and Westerveld *et al* (1979). For the higher ($n \geq 5$) lines of the $n^1P_1 \rightarrow 1^1S_0$ sequence the very recent measurement of Shemansky *et al* (1984) has been used. These cross section data are summarised in table 1 together with the XUV filter transmission at the corresponding wavelengths. The last column of table 1 gives the product of cross section and filter transmission. This number represents the contribution of each line to the detected He signal. The sum of this column, 1.329×10^{-19} cm^2, is equivalent to the total He fraction as seen by the detector. The measured He/He^+ ratio of 1.674 at 200 eV then leads to an equivalent for the He^+ contribution of 0.794×10^{-19} cm^2, assuming no wavelength variation in the channeltron efficiency.

Table 1. Helium reference data used in the normalisation procedure.

Transition wavelength (Å)	Cross section at 200 eV† (10^{-19} cm^2)	XUV filter transmission	Cross section × XUV filter transmission (10^{-19} cm^2)
$2^1P \rightarrow 1^1S$ 584	85.7‡	0.0072	0.617
$3^1P \rightarrow 1^1S$ 537	22.6‡	0.0147	0.331
$4^1P \rightarrow 1^1S$ 522	9.1‡	0.0175	0.159
$n \geq 5^1P \rightarrow 1^1S$ 517-505	11.1§	0.0200	0.222
			Σ: 1.329×10^{-19} cm^2

† Cascade included, corrected for polarisation.
‡ Average of cross section data given by van Eck and de Jongh (1970), Donaldson *et al* (1972) and Westerveld *et al* (1979).
§ Data from Shemansky *et al* (1984).

The detection efficiency of the channeltron does, however, depend on the wavelength of the incident VUV photon and so must be corrected for. The only published data appropriate to the 4039C channeltron which we used were by Weller and Young (1970) who quote quantum efficiencies of 0.105 and 0.143 at 304 Å and 584 Å, respectively, with an uncertainty of ±10%. Later work by Timothy and Bybee (1978) using different uncoated channeltrons is in essential agreement with these values. The use of these values automatically introduces a 20% systematic error into our 304 Å cross section. As a consequence of the lower detection efficiency for the He^+ compared with the He emissions we have to multiply the He^+ equivalent by a factor of 0.143/0.105 which leads to a value of 1.081×10^{-19} cm^2.

We estimate that 10% or 0.108×10^{-19} cm^2 of the total He^+ signal arises from the higher ^2P states. This estimate is based on previous measurements and calculations (Moustafa Moussa and de Heer 1967, Shemansky *et al* 1984) and is consistent with the near-threshold shape of our excitation function (figure 4), where a slight upward

trend was observed around 75 eV. The uncertainty in this correction leads to a small (2%) uncertainty in the final 304 Å cross section. The remaining 0.973×10^{-19} cm^2 transforms into a cross section of 6.20×10^{-19} cm^2 at 200 eV for the emission of the He^+ $2^2P \rightarrow 1^2S$ line at 304 Å, when the XUV filter transmission of 0.157 is taken into account. With a transmission of 0.220 at the shorter wavelengths, we find an emission cross section of 0.49×10^{-19} cm^2 for the combined shorter wavelength lines. Figure 5 shows our absolute emission cross section for the 304 Å line for impact energies from threshold to 300 eV together with the two previous absolute measurements. Our result is about 65% higher than the early experiment of Moustafa Moussa and de Heer (1967). Bloemen *et al* (1981) made only a single absolute measurement at 200 eV and suggested a renormalisation of their previously reported curve (Moustafa Moussa and de Heer 1967). Their result is close to our cross section and, in fact, the two measurements are well within each other's error bar. It should be noted that these cross sections include cascade contributions and are not corrected for any possible polarisation of the impact radiation.

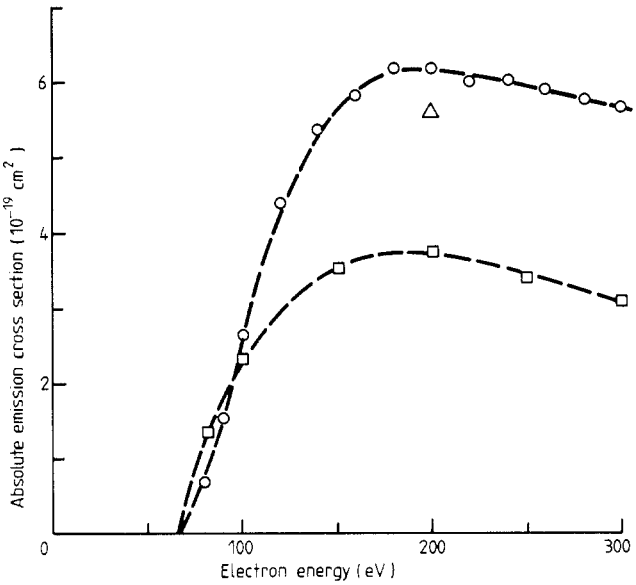

Figure 5. Absolute emission cross section of the He^+ 304 Å $2^2P \rightarrow 1^2S$ line as a function of electron energy. The different symbols refer to the present data (○), the experiment of Moustafa Moussa and de Heer (1967) (□), and the single measurement by Bloemen *et al* (1981) (△).

A quantitative statement on cascading is rendered difficult, since no reliable cross section data for individual transitions terminating on the 2^2P state are available. However, as the cross sections for exciting higher states in He^+ were found to decline very rapidly with increasing principle quantum number (see, e.g., Shemansky *et al* 1984), cascading is not expected to play an important role.

It is also difficult to estimate the effect of a possible polarisation of the 304 Å radiation on the cross section. In fact, only the polarisation of the $n = 4 \rightarrow n = 3$ manifold at 4686 Å has been measured (Elenbaas 1930, Haidt and Kleinpoppen 1966) and a threshold polarisation of 0.13 was found in the latter experiment. However, this result

is not relevant to our case, since the 4686 Å line is made up of all the allowed $l' \rightarrow l$ transitions, whereas the 304 Å line is a pure $P \rightarrow S$ ($l' = 1 \rightarrow l = 0$) transition. On the other hand, if it is assumed that the Percival-Seaton hypothesis (Percival and Seaton 1958) is applicable to the simultaneous ionisation-excitation process, a threshold polarisation of $P_{th} = 3/7 = 0.429$ and a high-energy limit of $P_\infty = -3/11 = -0.273$ should be expected for the subsequently emitted (unresolved) $2^2P_{1/2,3/2} \rightarrow 1^2S_{1/2}$ doublet. Note that He has zero nuclear spin and the polarisation is not attenuated by hyperfine structure perturbation. Such a strongly polarised emission would, of course, affect the shape of the measured 304 Å cross section through the anisotropy factor $(1 - P/3)$ where P is the energy-dependent polarisation. On the other hand, we do not expect the normalisation at 200 eV to be seriously affected, since in this energy range well away from threshold the polarisation is likely to be small. A polarisation fraction of 10% would lead to a 3% error in the cross section.

3.1.2. Sources of error. As mentioned before, the counting statistics in this experiment were 1% or better. Both the He target number density and the electron beam current are stable to 2%. The He cross section data taken from the three different sources agree to within 3% at 200 eV and there is an uncertainty of 1.5% introduced by the polarisation correction procedure. In addition, there is a further 2% error due to the uncertainty in the cross sections of the shorter wavelength ($\leq$517 Å) He lines and to the variation in the XUV filter transmission over this spectral range. This leads to a total uncertainty of 6.5% in the He reference data. The transmission of the XUV filter could be determined within an accuracy of 2% and a further 2% error is introduced as discussed earlier due to the uncertainty in the contribution from shorter wavelength ($\leq$256 Å) He^+ radiation. Combining these errors in quadrature leads to a total uncertainty of 8%. However, this error bar is more than tripled by the additional 20% uncertainty in the absolute quantum yield of the photon detector. Thus, at 200 eV impact energy, the cross section for emission of the He^+ $2^2P \rightarrow 1^2S$ line at 304 Å is $(6.2 \pm 1.7) \times 10^{-19}$ cm^2.

Clearly, it is the spread in the available data on the absolute quantum yield of the channeltron that limits the accuracy of our reported cross section. Therefore, as more accurate quantum yield data become available in the future, the accuracy of our 304 Å emission cross section will likewise improve.

3.2. The high-energy region

In the regime of high impact energies, a monochromator had to be used, as discussed earlier, to isolate the 304 Å line. Relative excitation function measurements were made for incident electron energies from 100–1000 eV. The shape in the overlap region (100–300 eV) was found to agree well with the curve of figure 5 when the relative excitation function was normalised at 200 eV. The result is shown in figure 6 with a few data points added from the low-energy measurement to complete the cross section curve (open squares). The corresponding data are listed in table 2. The product of cross section and impact energy is also included in figure 6 as a function of electron energy (open circles). It is obvious that the product of cross section and impact energy becomes a constant for incident electron energies above approximately 500 eV. This behaviour illustrates the optically forbidden nature of the simultaneous ionisation-excitation process as expected.

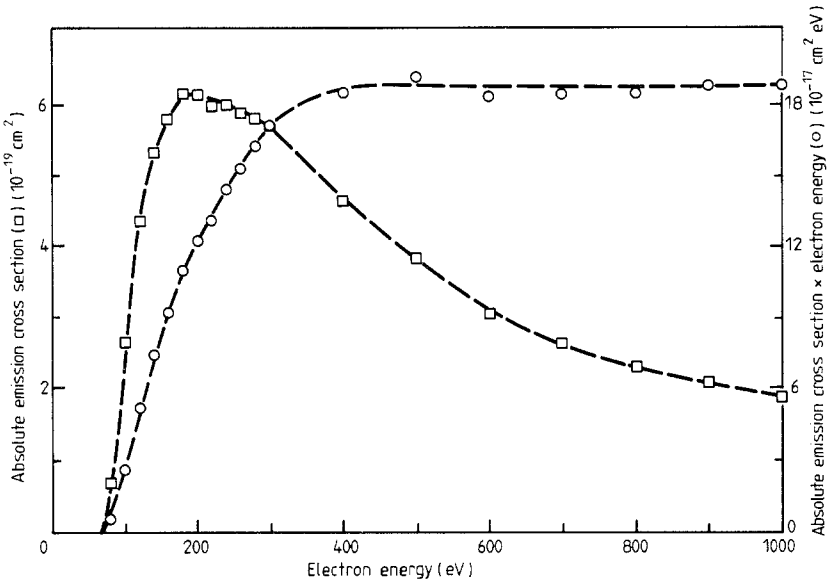

Figure 6. Absolute emission cross section of the He^+ 304 Å $2^2P \rightarrow 1^2S$ line as a function of electron energy (□). Also shown is the product of emission cross section and incident electron energy (○).

Table 2. Absolute emission cross section (not corrected for cascade or polarisation) of the He^+ $2^2P \rightarrow 1^2S$ line at 304 Å.

Electron energy (eV)	Emission cross section (10^{-19} cm^2)
80	0.7
90	1.5
100	2.7
120	4.4
140	5.4
160	5.9
180	6.2
200	6.2
220	6.0
240	6.0
260	5.9
280	5.9
300	5.8
400	4.7
500	3.9
600	3.1
700	2.7
800	2.3
900	2.1
1000	1.9

4. Summary

We have presented a simple and straightforward approach to measure the cross section for emission of the He^+ $2^2P \rightarrow 1^2S$ line at 304 Å following electron impact on He. A value of $(6.2 \pm 1.7) \times 10^{-19}$ cm^2 at 200 eV impact energy was found which is in good agreement with the $(5.6 \pm 1.4) \times 10^{-19}$ cm^2 reported by Bloemen *et al* (1981). Since the current lack of reliable quantum yield data for the photon detector which was used in our experiment accounts for 70% of our total uncertainty, a detailed discussion of the normalisation procedure and the errors involved is given. Once high-accuracy quantum yield and polarisation data become available, our experiment will provide the basis for a 304 Å cross section with an error margin of less than 10%. This would greatly improve the applicability of this cross section as a reliable calibration standard in the extreme ultraviolet. Polarisation measurements on the $n^2P \rightarrow 2^2S$ transitions of He^+ are currently underway in our laboratory. These will be particularly helpful in establishing the low-energy shape of the excitation functions where the polarisation fraction of the radiation is likely to be highest.

Acknowledgments

The authors gratefully acknowledge financial assistance from the Natural Sciences and Engineering Research Council of Canada (NSERC). J W McConkey acknowledges the hospitality of the Jet Propulsion Laboratory, California Institute of Technology, during the period when this manuscript was being prepared for publication.

We wish to thank Dr J M Ajello for making his results available to us prior to publication.

References

Becker K and McConkey J W 1984 *Can. J. Phys.* **62** 1-9
Becker K, van Wijngaarden W and McConkey J W 1983 *Planet. Space Sci.* **31** 197-206
Bethe H A 1930 *Ann. Phys., Lpz.* **5** 325
Bloemen E W P, Winter H, Mark T, Dijkkamp D, Barrends D and de Heer F J 1981 *J. Phys. B: At. Mol. Phys.* **14** 717-25
Donaldson F G, Hender M A and McConkey J W 1972 *J. Phys. B: At. Mol. Phys.* **5** 1192-210
Elenbaas W 1930 *Z. Phys.* **59** 289-305
Haidt D and Kleinpoppen H 1966 *Z. Phys.* **196** 72-6
Heddle D W O and Keesing R G W 1968 *Adv. At. Mol. Phys.* **4** 267-98
Heddle D W O and Lucas C B 1963 *Proc. R. Soc.* A **271** 129-35
Lee E T P and Lin C C 1965 *Phys. Rev.* **138** A301-4
Moustafa Moussa H R and de Heer F J 1967 *Physica* **36** 646-54
Percival I C and Seaton M J 1958 *Phil. Trans. R. Soc.* **251** 113-38
Shemansky D E, Ajello J M, Hall D T and Franklin B 1984 private communication
Striganov A R and Sventitskii N S 1968 *Tables of Spectral Lines of Neutral and Ionized Atoms* (New York: Plenum)
Sutton J F and Kay R B 1974 *Phys. Rev.* A **9** 697-703
Timothy J G and Bybee R L 1978 *Rev. Sci. Instrum.* **49** 1192-6
van Eck J and de Jongh J P 1970 *Physica* **47** 141-58
Weller C S and Young J M 1970 *Appl. Opt.* **9** 505-6
Westerveld W B, Heideman H G and van Eck J 1979 *J. Phys. B: At. Mol. Phys.* **12** 115-35